Dendritic Models of Redox Proteins: X-Ray Photoelectron Spectroscopy and Cyclic Voltammetry Studies of Dendritic Bis(terpyridine) Iron(II) Complexes

Hak-Fun Chow,* Ida Y.-K. Chan, Dominic T. W. Chan, and Raymund W. M. Kwok

Abstract: A series of iron-containing metallodendrimers from the zeroth to the third generation was synthesized and characterized. The iron(II) ion of these metal complexes is encapsulated within a hydrophobic polyether dendritic envelope. X-ray photoelectron spectroscopy analysis revealed that the bonding environment of the iron atom was essentially the same in dendrimers of different generations. However, cyclic voltammetry studies indicated that the reversibility of the metal redox process decreased in the higher-generation dendrimers. These observations were similar to those of a related electrochemical study conducted on the redox protein cytochrome C, in which the decrease in electron transfer reversibility was explained as a result of the increasing remoteness of the metal ion of the higher-generation dendrimers from the electrode surface.

Keywords
cyclic voltammetry · dendrimers · metallodendrimers · terpyridine · X-ray photoelectron spectroscopy

Research in dendrimer chemistry has moved on from the initial efforts devoted to dendrimer synthesis and investigations of structural properties.[1] Emphasis in this area has recently been switched to the exploration of the practical use of functionalized dendritic molecules,[2] and the potential of these hyperbranched molecules in molecular recognition, biological modeling, and catalyst applications has begun to emerge. Instead of looking at the global properties of dendritic molecules, studies are now focused on the change of photophysical/photochemical,[3] electrochemical,[4] optical,[5] host-guest encapsulation,[6] and catalytic properties[7] when simple functional units (e.g., photoactive, redox-active, or catalytic) are attached to a dendritic matrix.

Hyperbranched dendrimers, in contrast to simple polydisperse long-chain polymers, are unique macromolecular models for the study of a wide range of biological processes. Because they are monodisperse and have a highly ordered architecture, the properties of functional dendrimers can be easily correlated to their molecular dimension and topology. They are ideal artificial models of biomolecules such as proteins and enzymes and can be used to mimic biological processes that are inaccessible with lower molecular weight models. By attaching simple functional groups to different positions of a dendritic matrix, one can set up different types of biological models and study the various kinds of macromolecular interactions. For example, the functional group may be encapsulated inside a dendritic envelope, thus providing a good opportunity to investigate the internal properties of the dendrimer by observing the property change of the functional group of interest. The dendritic zinc porphyrin system recently disclosed by Diederich[4a, c] represented one of the pioneering works looking at the change of redox behaviour of the zinc ion upon dendrimerization. Alternatively, a dendritic model with the functional group located on the exterior surface permits an evaluation of the influence of the dendritic surface on the properties of the functional moiety. For instance, Brunner[7a] reported the modulation of catalytic reactivity of a novel series of catalytic dendrimers (dendrizymes) by attaching chiral groups on a bisphosphine ligand. More interestingly, if more than one functional group is attached to a dendritic matrix, the resulting entity is an ideal model for studying cooperation or allosteric interactions between these functional units. For example, negative catalytic cooperation of a dendrizyme with multiple arylnickel(II) catalytic centers has been observed by van Koten.[7d]

Amongst these modeling processes, the modulation of physicochemical properties of the interior functional core by the dendritic envelope is of particular interest. This effect is similar to that of the polypeptide scaffolding of an enzyme molecule that provides the chiral and substrate-specific environment for the reactive functional groups inside the active site. With regard to redox-active proteins, the polypeptide surfaces function as important determinants for the specificity of electron transfer by defining the positions of the redox centers and the electron-transfer pathways.[8] In contrast to enzyme or protein molecules, in which the three-dimensional environment of the catalytic pocket is engineered by the amino acid sequence, the synthesis of functional dendrimers with a predefined three-dimensional structure has been a challenge. Fortunately, recent advances in dendrimer synthesis facilitate the incorporation of specific functional groups at predefined positions within a dendritic matrix.[9] As a result, a number of novel metalloden-

Prof. Dr. R. W. M. Kwok
Department of Chemistry, The Chinese University of Hong Kong
Shatin, NT (Hong Kong)
Fax: Int. code +2603-5057
e-mail: b381765@idea.csc.cuhk.hk

 0947-6539/96/0209-1086 $ 15.00+.25/0

drimers with the metal ion situated in the interior of the dendritic structure have recently appeared. These dendritic systems were designed to model the electron-transfer process of redox proteins. For example, it was discovered that electron-rich dendritic fragments attached to zinc porphyrin facilitated oxidation but disfavored reduction of the zinc ion.[4a] Most intriguingly, the redox potential of zinc porphyrin could also be modulated by the environmental polarity.[4c] On the other hand, a hydrocarbon dendritic envelope was reported to decrease the reversibility of the redox process of bis(terpyridine) ruthenium(II) complexes.[4b] These examples show that metallodendrimers are interesting mimics for metalloproteins and the dendritic envelope does affect the redox properties of the metal ion of interest. In this paper we disclose our own studies on the changes in solubility and redox properties of a series of hexacoordinated iron(II) complexes in which the metal ion is encapsulated between two compact polyether-based dendritic terpyridine (terpy) ligands of the types **1**–**4** (Fig. 1). We also report here the use of X-ray photoelectron spectroscopy to study the structure and electron-transfer processes of these macromolecular complexes in the solid state.

Results and Discussion

Several terpyridine-based metallodendrimers have been reported in the past, notably those of Newkome and Constable,[4b, 10] but the study of their electrochemical properties has been limited to those of the ruthenium(II) complexes. The study by Newkome[4b] showed that the decrease in reversibility of the metal redox process towards higher-generation dendrimers could be attributed to the increasing steric destabilization of the oxidation and reduction states of the higher-generation metallodendrimers. In Newkome's example, the ruthenium(II) ion was encapsulated between two dendritic terpy ligands, one of which contained a flexible long-chain hydrocarbon spacer between the terpy and the dendritic moieties. As a result, the metallodendrimer had a relatively flexible and open structure. Hence it is difficult to address the steric environment around the ruthenium center, especially its distance from the two polyamide dendritic envelopes. Our aim is to sandwich a metal ion in a structurally rigid and sterically compact dendritic matrix. The absence of a flexible hydrocarbon link in our models could reduce the conformational flexibility of the dendritic moieties with respect to their positions around the iron center and allows us to attribute the redox property change to the molecular dimension of the dendritic fragment more precisely.

Synthesis: The dendritic terpy ligands **1**–**4** consist of two components: the terpy moiety for metal complexation and a polyether-based dendritic component.[11] The dendritic sectors **5**–**8** have the advantage of being stable in both acidic and basic media. Moreover, they do not show any redox process from −2.0 to 1.9 V in cyclic voltammetry studies[11] and therefore enable us to study the electrochemical properties of the resulting metallodendrimers without interference from the dendritic matrix.

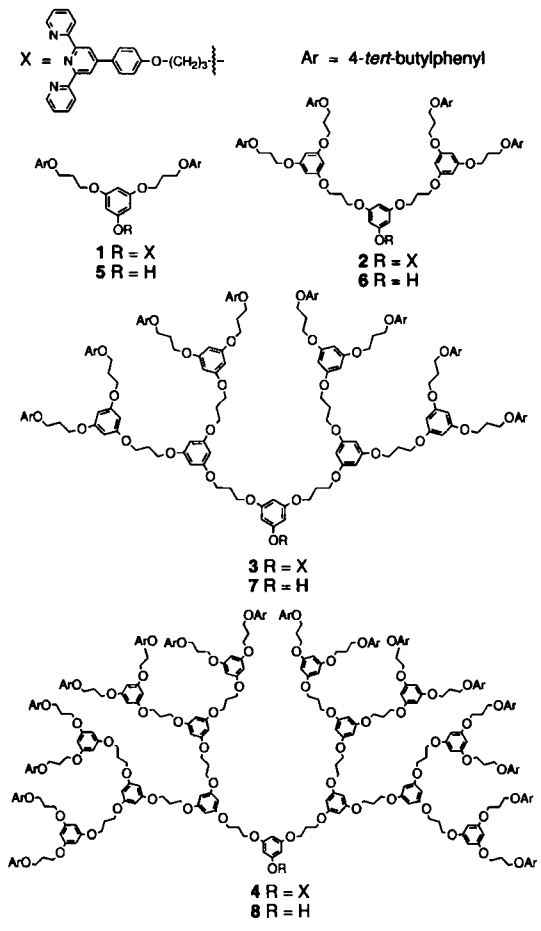

Fig. 1. The dendritic terpyridine ligands **1**–**4** and the dendritic sectors **5**–**8**.

The starting point for the synthesis of the terpy core was the 4-substituted benzaldehyde **9** (Scheme 1), which could be prepared from commercially available 4-hydroxybenzaldehyde by coupling to 3-bromopropanol in the presence of potassium carbonate in acetone. The benzaldehyde derivative **9** was then con-

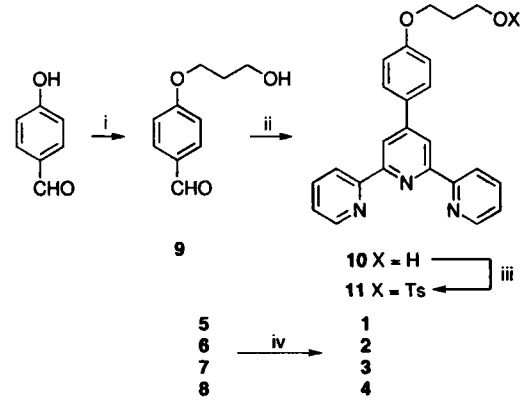

Scheme 1. Synthesis of dendritic terpyridine ligands. i) 3-bromopropanol, K_2CO_3; ii) 2-acetylpyridine, $MeCONH_2$, NH_4OAc; iii) TsCl, pyridine; iv) **11**, K_2CO_3, acetone/DMF.

Abstract in Chinese:

本文报导一系列金属树枝状分子的合成和结构鉴定，该系分子为铁(II)离子的络合物，配位体由三联吡啶及从零伸展至第三世代的苯环及烷氧桥互扣的树枝体组成。此种络合物的铁离子均被封闭於一个厌水性的树枝状有机体内，结构特殊。X射线光电图显示有关的铁离子在不同世代衍生出的配位体内，化学耀性质大致相同，但循环伏安实验则显示高世代配位体络合的铁离子之氧还反应可逆性随世代数目增加而减低，後者实验结果和氧化蛋白细胞色素C的电化学颇为相似。电子传递可逆性的渐降现象可能是由於在高世代树枝状分子内的铁离子逐渐远离电极表面所致。

0947-6539/96/0209-1086 $ 15.00+.25/0 Chem. Eur. J. 1996, 2, No. 9

verted to the 2,2′:6′,2″-terpy derivative **10** in one pot as described in the literature.[12] As expected, a 4:1 mixture of the desired terpy **10** and its 2,2′:4′,2″-isomer was formed, which were readily purified by a metal complexation–decomplexation procedure.[13] Subsequent conversion of the primary hydroxy group to the corresponding *p*-toluenesulfonate **11** was effected by treatment of **10** with toluene sulfonyl chloride in the presence of pyridine. This sulfonate **11** could then be used to connect to the polyether dendritic sectors **5**–**8** of different generations.

The synthesis of the polyether-based dendritic phenols of different generations **5**–**8** has been described elsewhere.[11] Coupling of zeroth-generation dendritic fragment **5** to the core **11** in the presence of K_2CO_3 in acetone proceeded smoothly to give the zeroth-generation terpy ligand **1** (**G0**) in 80% yield. The assembly of the higher-generation dendritic sectors **6**–**8** onto the terpy moiety **11** required the presence of DMF as a cosolvent to accelerate the reaction. Thus the ligands **2**–**4** (**G1**–**G3**), from the first to the third generations, could be obtained in 96, 90, and 89% yields, respectively, from **6**–**8**. For comparison purposes, a nondendritic terpy ligand **12** was also synthesized in 76% yield by coupling **11** to *tert*-butyl phenol (Scheme 2).

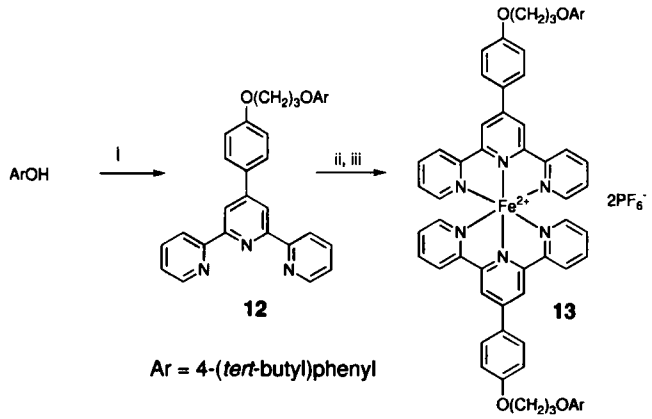

Scheme 2. Synthesis of metal complex **13**. i) **11**, K_2CO_3; ii) $FeCl_2 \cdot 4H_2O$; iii) NH_4PF_6.

The final step of our synthetic sequence involved complexation of the dendritic ligands with the iron(II) ion. Treatment of the nondendritic terpy ligand **12** with $FeCl_2 \cdot 4H_2O$ in methanol afforded a deep purple complex $[Fe(\mathbf{12})_2]^{2+}$. Precipitation of this complex with NH_4PF_6 afforded the hexafluorophosphate salt $[Fe(\mathbf{12})_2][PF_6]_2$ (**13**) in 67% yield as a purple crystalline solid. By the same procedure, $[Fe(\mathbf{1})_2][PF_6]_2$ (**14**) could be obtained in 65% yield as a purple crystalline solid. The dendritic ligands of higher generations proved to be insoluble in boiling methanol and therefore a mixture of chloroform and ethanol was used as the reaction solvent. In this manner, $[Fe(\mathbf{2})_2][PF_6]_2$ (**15**), $[Fe(\mathbf{3})_2][PF_6]_2$ (**16**), and $[Fe(\mathbf{4})_2][PF_6]_2$ (**17**) were synthesized as purple amorphous solids from **2**, **3**, and **4** in 82, 79, and 80% yields, respectively.

Structural characterization: The structural identities of these metallodendrimers were confirmed by ^1H, ^{13}C NMR, mass spectrometry and elemental analysis. The presence of the doubly charged molecular ion $Fe(terpy)_2^{2+}$ in the mass spectra provided strong evidence that these metallodendrimers formed were the bis(terpy) iron(II) complexes instead of the rarely isolated reddish-purple mono(terpy) iron(II) complexes.[14] As expected, on going from the lower to the higher generations, the ^1H and ^{13}C NMR spectra showed a gradual decrease of signal intensities arising from the terpyridine core relative to the dendritic aromatic and aliphatic envelope signals (Figs. 2 and 3). We know

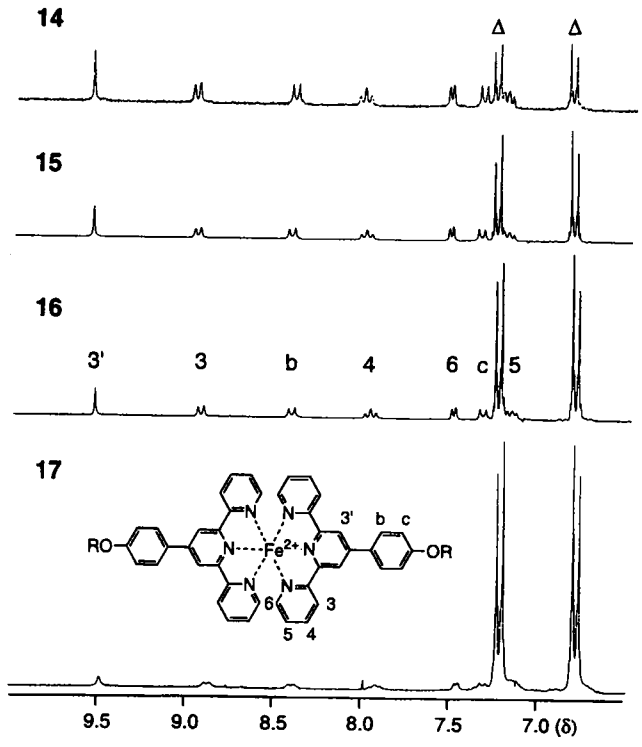

Fig. 2. ^1H NMR spectra showing the aromatic region (δ = 10.0–6.5) of iron(II) terpyridine complexes **14**–**17** (Δ denotes signals arising from the polyether dendritic sectors).

these metallodendrimers also exist as the bis(terpy) complexes in the solution state because their ^1H NMR spectra consist of sharp signals. The high spin mono(terpy) complexes are paramagnetic[14] and much signal broadening in their ^1H NMR spectra would have appeared.

Solubility properties: In contrast to lower molecular weight bis(terpy) iron(II) complexes, which are readily soluble in polar solvents but only slightly in chlorinated solvents, the metallodendrimers **14**–**17** are readily soluble in chloroform, acetone, and THF, but not in polar solvents such as acetonitrile or alcohols despite their ionic character. The hydrophobic environment associated with these metallodendrimers **14**–**17** probably forces the counteranion PF_6^- to form a tight ion pair with the iron(II) ion within the hydrocarbon dendritic envelope. The ionic nature of these macromolecular complexes in solution is thus masked and leads to a change in their solubility properties.

X-ray photoelectron spectroscopic studies: The metallodendrimers were examined by X-ray photoelectron spectroscopy (XPS) to provide information regarding the electron structure and chemical environment of the core electrons in the solid state. Samples were prepared as a thin-layer disc placed on aluminum foil and subjected to X-ray photoelectron analysis. All the basic atomic constituents of the metallodendrimers could be

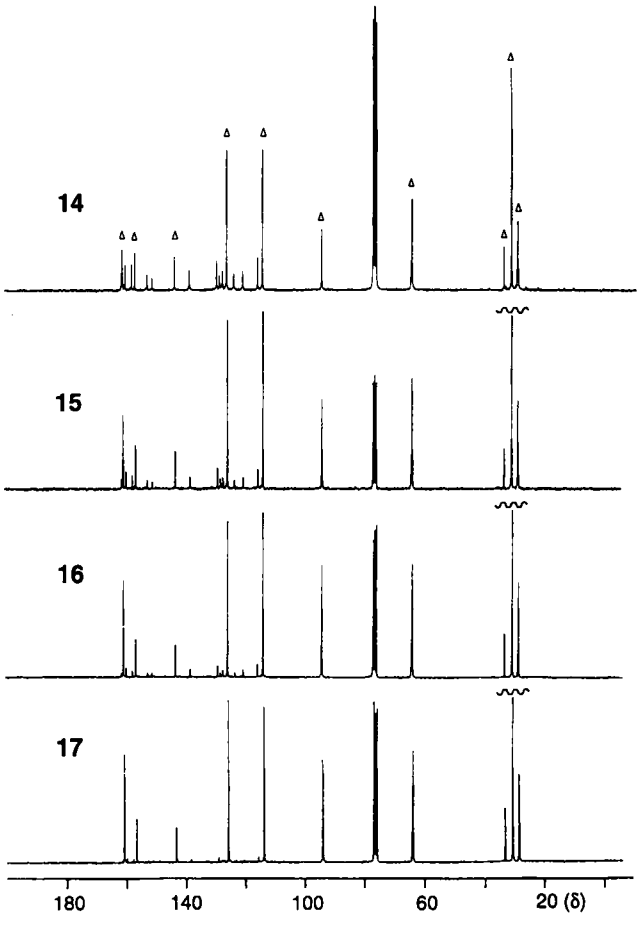

Fig. 3. ^{13}C NMR spectra of iron(II) terpyridine complexes **14**–**17** (Δ denotes signals arising from the polyether dendritic sectors).

identified in the region scans except for the third-generation complex $[Fe(4)_2][PF_6]_2$ (**17**), in which the peak for the iron 2p photoelectron could not be detected (Table 1 and Fig. 4). This could be a result of the extremely low percentage of iron content

Table 1. XPS results (eV) for iron(II) complexes **13**–**17** [a].

Metallodendrimers	Binding energies						Difference
	C 1s	N 1s	O 1s	Fe 2p	P 2p	F 1s	(Fe 2p – N 1s)
$[Fe(12)_2][PF_6]_2$ (**13**)	287.0	401.7	534.7	710.4	138.2	688.0	308.7
$[Fe(1)_2][PF_6]_2$ (**14**)	287.5	401.7	535.0	710.6	138.1	688.3	308.9
$[Fe(2)_2][PF_6]_2$ (**15**)	287.0	401.7	534.7	710.5	139.8	688.1	308.8
$[Fe(3)_2][PF_6]_2$ (**16**)	287.0	401.7	534.5	710.5	139.5	688.0	308.8
$[Fe(4)_2][PF_6]_2$ (**17**)	287.2	401.7	534.7	–	139.4	688.1	–

[a] Only the relative peak positions are meaningful because of surface charging. All values are reported relative to the binding energy of the N 1s orbital, which is set at 401.7 eV.

in this molecule, leading to an insignificant signal. Another possible factor is that the iron atom is buried deep inside the macromolecule, resulting in a higher probability that the escaped electron is scattered by the surrounding matter and thus diminishing the iron 2p photoelectron signal intensity. Owing to the increasing oxygen content, the oxygen 1s signal became more prominent than the carbon 1s signal in the XPS spectra of the higher-generation dendrimers. The decreasing relative fluorine, iron, nitrogen, and phosphorus contents in the higher generations were also reflected by their diminishing signals in the corresponding spectra. It was also found that the difference in binding energies between the nitrogen 1s and iron 2p electrons remained essentially the same (309 eV) in metallodendrimers of different generations. Since the binding energy of a particular atom is sensitive to its oxidation state, and in particular to its net charge, this result suggests that the coordinating environments of the metal ion in different generations are very similar irrespective of the increasing size and molecular weight of the ligands.

Cyclic voltammetry studies: The results of cyclic voltammetry studies of these metallodendrimers provided useful information regarding the redox properties of the molecules in the solution state (Table 2). The nondendritic and lower-generation metallodendrimers **13**–**15** (Fig. 5) exhibited one oxidation [Fe(II) → Fe(III)] (E ca. 1.0 V) and two reduction [Fe(II) → Fe(I) and Fe(I) → Fe(0)] (E ca. −1.3 and −1.5 V) processes.

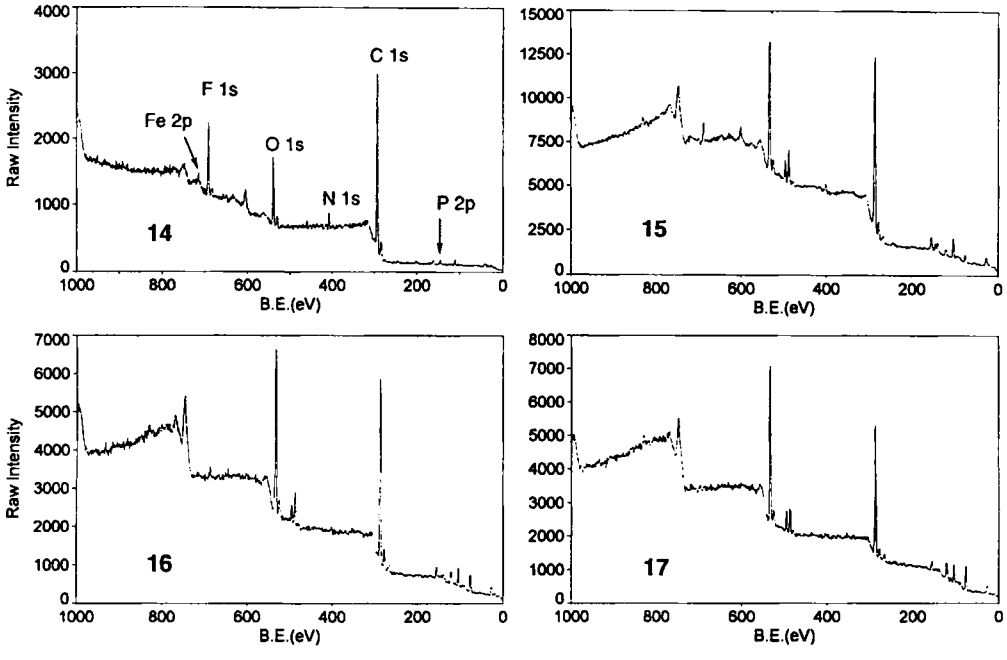

Fig. 4. X-ray photospectroscopic spectra (survey scan) of iron(II) terpyridine complexes **14**–**17**.

0947-6539/96/0209-1088 $ 15.00+.25/0 Chem. Eur. J. 1996, 2, No. 9

Table 2. Cyclic voltammetry data (calibrated against ferrocene as internal standard): $E^{1/2}$ [approximated by $(E_{pc} + E_{pa})/2$] in V; $\Delta E (E_{pa} - E_{pc})$ in mV. Experimental conditions: sweep rate 100 mVs^{-1}, supporting electrolyte $Bu_4N^+BF_4^-$, Ag reference electrode, platinum working and counter electrodes, 23 °C.

Metallodendrimers	$E_{ox}^{1/2}$ (ΔE)	$E_{red}^{1/2}$ (I) (ΔE)	$E_{red}^{1/2}$ (II) (ΔE)
$[Fe(terpy)_2][ClO_4]_2$ [a]	1.09	−1.26	−1.41
13 [b]	1.03 (80)	−1.27 (80)	−1.38 (70)
14 [c]	1.02 (130)	−1.29 (110)	−1.48 (120)
15 [c]	1.02 (200)	−1.29 (140)	−1.47 (130)
16	1.12 [d,e]	−1.36 [c,e]	
17	– [d,f]	−1.37 [c,e]	

[a] Solvent: MeCN; supporting electrolyte: $Et_4N^+PF_6^-$; see ref [15]. [b] In MeCN. [c] In CH_2Cl_2. [d] In THF. [e] Poorly resolved signal. [f] No signal observed.

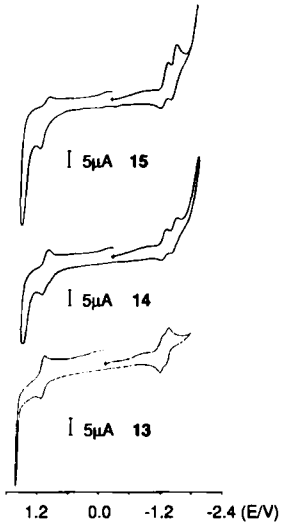

Fig. 5. Cyclic voltammograms of **13**–**15**.

The average peak potentials $[(E_{pc} + E_{pa})/2]$ of these three processes were essentially the same across the zeroth and first generations and were comparable to those of non-dendritic complex **13** and $[Fe(terpy)_2][ClO_4]$,[15] indicating that there is little change of the metal redox properties of these species upon dendrimerization to lower-generation sectors. This finding was similar to the cyclic voltammetry results of the ruthenium(II) metallodendrimers reported by Newkome,[4b] but was different from that of the zinc(II) dendritic porphyrin disclosed by Diederich,[4a] in which a shift of the oxidation and reduction potentials of the zinc metal was observed when the central metalloporphyrin was enclosed within an electron-rich dendritic coating. The peak separation (ΔE) of the oxidation process increased by 50 and 120 mV on moving from the non-dendritic iron(II) complex **13** to the zeroth and first-generation metallodendrimers **14** and **15**, respectively. Thus, the reversibility of the redox reaction decreased with increasing generation number; this observation was in line with Newkome's results. A similar trend was also observed for the two reductive processes, although the decrease in reversibility occurred to a lesser extent, as indicated by a smaller peak separation (ΔE) value.

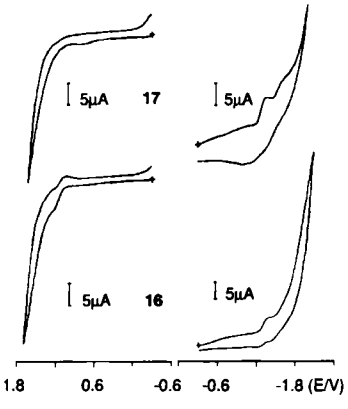

Fig. 6. Cyclic voltammograms of **16** and **17** (left: oxidation; right: reduction).

Irreversibility of the electron-transfer process was first noticed in our second-generation homoleptic metallodendrimer **16**, with one irreversible oxidation potential at 1.12 V and one irreversible reduction at −1.36 V (Fig. 6). The third-generation complex **17** exhibited no defined oxidative wave but one irreversible reduction process at approximately −1.37 V. Because of their irreversible nature, these signals were poorly resolved and the errors associated with the reported redox potentials were high. It was noteworthy that irreversibility was first observed in our second-generation dendrimer, whereas Newkome's group first noticed irreversibility in their 1:4-tiered heteroleptic ruthenium(II) complex. In contrast, the reaction of their 2:3-tiered ruthenium complex was electrochemically and chemically reversible.

The bonding and electronic nature of the iron(II) center were essentially the same across the different generations, as indicated by XPS studies, where the peak separation between the nitrogen 1s and iron 2p signals remained nearly constant. This was also supported by CV results obtained from the lower-generation metallodendrimers. The decrease in reversibility of the redox transfer for the higher-generation dendrimers as compared with the lower ones in CV studies is of particular interest. It was previously suggested that the decrease in reversibility in the redox process was due to the increased steric hindrance of the higher-generation metallodendrimers, leading to the facile decomposition of the metal complex upon oxidation or reduction.[4b] Direct electrochemical studies of redox proteins[16] such as cytochrome C pointed out that protein molecules must bind reversibly to the electrode surface in order to achieve efficiently fast electron transfer. Moreover, even if the protein is adsorbed on the electrode, if the distance between its redox center and the surface of the electrode exceeds the distance across which electrons can be transferred at measurable rate, the rate of electron transfer is still minimal.[17] We believe that the polyether dendritic sector serves as an insulating coating for the iron(II) redox center, which was located deep inside the macromolecular complexes. For the higher-generation metallodendrimers, the increasing remoteness of the iron(II) ion from the electrode surface hinders the electron-transfer process and leads to the broadening of the CV waves and the decrease in reversibility. Furthermore, the different degree of compactness of the dendritic coating around the metal center could also affect the reversibility of the redox reaction. Owing to the absence of the long C_{12} hydrocarbon spacer between our dendritic sectors and the terpyridine core, our metal ion is probably more tightly sealed in than those of Newkome. Hence, irreversibility of the redox behaviour appeared earlier in our dendritic series.

Conclusions

We have reported here the details of the preparation and characterization of a series of iron(II)-containing metallodendrimers with increasing molecular dimensions. The metal ion is located in the interior of a polyether dendritic matrix. The redox properties of these metallodendrimers in the solid and solution states were examined by XPS and CV techniques, with the aim of modeling the electron-transfer process of redox-active metalloproteins in nature. It was shown that the dendritic organic coating could alter the solubility and redox properties of the metal complexes. The size (dendrimer generation) and shape (degree of compactness) of the dendritic sectors were discovered to be important determinants for the specificity of the electron-transfer process. The redox reaction of the metal ion became increasingly irreversible as the thickness of the dendritic coating increased. This decrease in reversibility of the electron transfer at the metal center for higher-generation metallodendrimers can be rationalized by the increasing remoteness of the redox center from the electrode surface.

Experimental Section

Melting points were measured on a Reichert Microscope apparatus and are uncorrected. ^{1}H (250 MHz) and ^{13}C (62.9 MHz) NMR spectra were acquired on a Bruker WM 250 spectrometer. IR spectra were recorded on a Nicolet 205 FT-IR spectrometer as film on KBr discs. Mass spectra were obtained on a Bruker APEX 47e FTMS with liquid secondary-ion mass spectrometry (L-SIMS) or electrospray ionization (ESI) techniques. The reported molecular mass (m/z) values, unless otherwise specified, were monoisotopic mass. Elemental analyses were carried out at MEDAC (UK). UV/visible spectra were recorded on a Hitachi U-2000 spectrometer. Electrochemical studies were carried out with a EG&G PAR Model 173 Potentiostat, Model 175 Universal Programmer, and Model RE0089 X-Y Recorder. The working, counter, and reference electrodes were made of a platinum disc, platinum, and silver, respectively, and were polished with alumina immediately before use. Dry nitrogen was bubbled through samples for 3 min before CV experiments. Tetrabutylammonium tetrafluoroborate was used as supporting electrolyte. Cyclic voltammograms were obtained at scan rate of 100 mVs^{-1}. X-ray photoelectron spectroscopy (XPS) studies were performed on a Kratos AXIS-HS X-ray photoelectron spectrometer ($Mg_{K\alpha}$, 1253.6 eV). Unless otherwise stated, all chemicals were purchased from commercial suppliers and used without further purification. Tosyl chloride was recrystallized from toluene before use. Dichloromethane, *N,N*-dimethylforamide, and acetonitrile were distilled from P_2O_5 and stored over 4 Å molecular sieves. Tetrahydrofuran (THF) was freshly distilled over sodium/benzophenone. Tetrabutylammonium tetrafluoroborate (TBAF) was dried under vacuum for 1 day prior to use. Neutral alumina (activity II) was used for chromatographic separation of terpyridine ligands and their corresponding iron(II) complexes.

4-(3-Hydroxypropoxy)benzaldehyde (9): A mixture of 3-bromopropanol (11.4 g, 82.0 mmol), 4-hydroxybenzaldehyde (10.0 g, 82.0 mmol) and potassium carbonate (22.6 g, 164 mmol) was refluxed in acetone (100 mL) for 30 h. The mixture was filtered and the filtrate concentrated in vacuo to give the crude product. Flash chromatography on silica gel (hexane/EtOAc = 2/1 gradient to 5/3) afforded **9** [18] (10.2 g, 69%) as a colorless oil; R_f = 0.18 (hexane/Et_2O = 1/1); ^{1}H NMR ($CDCl_3$): δ = 9.75 (s, 1H; CHO), 7.72 (d, ^3J(H,H) = 8.8 Hz, 2H; Ar–H), 6.91 (d, ^3J(H,H) = 8.8 Hz, 2H; Ar–H), 4.11 (t, ^3J(H,H) = 6.1 Hz, 2H; CH_2OAr), 3.78 (t, ^3J(H,H) = 6.1 Hz, 2H; CH_2OH), 3.10–2.90 (brs, 1H; OH), 2.00 (quin, ^3J(H,H) = 6.1 Hz, 2H; CCH_2C).

4′-[4-(3-Hydroxypropoxy)phenyl]-2,2′:6′,2″-terpyridine (10): A mixture of 2-acetylpyridine (6.9 g, 57 mmol), acetamide (41 g, 390 mmol), ammonium acetate (30 g, 690 mmol), and the aldehyde **9** (5.2 g, 29 mmol) was refluxed at 180 °C for 3 h. After addition of sodium hydroxide solution (24 g NaOH in 48 mL water), the mixture was heated at 120 °C for 2 h without stirring. The mixture was poured into water and extracted with dichloromethane (3 × 80 mL). The organic layer was dried ($MgSO_4$), filtered, and concentrated to give the crude product. Flash chromatography on alumina (hexane/$CHCl_3$ = 3/2 gradient to 3/4) gave a mixture of **10** and the 2,2′:4′,2″-regioisomer as a yellow solid. This solid was redissolved in methanol (30 mL) and $FeCl_2 \cdot 4H_2O$ (1.81 g, 9.10 mmol) was added. The mixture was refluxed for a further 3 h, and a solution of NH_4PF_6 (3.0 g, 18.2 mmol) in methanol (5 mL) was added to give a deep purple precipitate. This precipitate was collected and washed with dichloromethane (100 mL). The desired terpy ligand **10** (2.8 g, 25%) was then regenerated as a light yellow solid by treating the purple complex with 30% H_2O_2 (5 mL) in a mixture of acetonitrile (10 mL) and aqueous NaOH solution (4 mL) following a literature procedure [13]; m.p. 91–93 °C; R_f = 0.51 (hexane/EtOAc = 1/1); ^{1}H NMR ($CDCl_3$): δ = 8.74–8.65 (m, 4H), 8.69 (s, 2H), 7.87 (d, ^3J(H,H) = 8.8 Hz, 2H), 7.87 (dt, ^4J(H,H) = 1.9 Hz and ^3J(H,H) = 7.6 Hz, 2H), 7.35 (ddd, ^3J(H,H) = 7.6 Hz, ^3J(H,H) = 4.8 Hz and ^4J(H,H) = 1.2 Hz, 2H), 7.02 (d, ^3J(H,H) = 8.9 Hz, 2H), 4.17 (t, ^3J(H,H) = 6.0 Hz, 2H; CH_2OAr), 3.89 (t, ^3J(H,H) = 6.0 Hz, 2H; CH_2OH), 2.08 (quin, ^3J(H,H) = 6.0 Hz, 2H; CCH_2C), 1.85 (brs, 1H; OH); ^{13}C NMR ($CDCl_3$): δ = 159.9, 156.5, 155.9, 149.7, 149.1, 136.8, 131.0, 128.5, 123.7, 121.4, 118.3, 115.0, 65.7 (CH_2O), 60.2 (CH_2O), 32.2 (CCH_2C); IR (film): $\tilde{\nu}$ = 3367 (OH), 1608, 1585, 1568, 1515 cm^{-1}; MS (EI): m/z (%) = 383 (77) [M^+] and 325 (100) [$M^+ - C_3H_6O$]; $C_{24}H_{21}N_3O_2$ (383.5) calcd C 75.18, H 5.52, N 10.96; found C 74.70, H 5.46, N 10.60.

4′-[4-(3-Tosyloxypropoxy)phenyl]-2,2′:6′,2″-terpyridine (11): A mixture of the alcohol **10** (0.83 g, 2.2 mmol), tosyl chloride (2.0 g, 10 mmol), and pyridine (3.3 mL, 48 mmol) was stirred at room temperature in dried dichloromethane (25 mL) for 3 d. Excess pyridine was evaporated in vacuo and the residue redissolved in dichloromethane (50 mL). The solution was washed with Na_2CO_3 (20 mL) and NaCl solution (20 mL). The organic layer was dried ($MgSO_4$), filtered, and evaporated in vacuo to give a solid which was recrystallized from $CHCl_3$/hexane (2/5) to give tosylate **11** (0.83 g, 71%) as a white crystalline solid; m.p. 144–145 °C; R_f = 0.22 (hexane/$CHCl_3$ = 10/3); ^{1}H NMR ($CDCl_3$): δ = 8.73–8.65 (m, 4H), 8.69 (s, 2H), 7.90–7.81 (m, 4H), 7.75 (d, ^3J(H,H) = 8.3 Hz, 2H), 7.35 (dd, ^3J(H,H) = 7.2 Hz and ^3J(H,H) = 4.9 Hz, 2H), 7.23 (d, ^3J(H,H) = 7.9 Hz, 2H), 6.86 (d, ^3J(H,H) = 8.7 Hz, 2H), 4.26 (t, ^3J(H,H) = 6.0 Hz, 2H), 3.99 (t, ^3J(H,H) = 5.8 Hz, 2H), 2.34 (s, 3H; CH_3), 2.14 (quin, ^3J(H,H) = 5.9 Hz; CCH_2C); ^{13}C NMR ($CDCl_3$): δ = 159.4, 156.3, 155.9, 149.6, 149.0, 144.7, 136.8, 133.0, 131.0, 129.8, 128.4, 127.8, 123.7, 121.3, 118.2, 114.8, 66.9, 63.3, 28.9, 21.5; IR (film): $\tilde{\nu}$ = 1608, 1584, 1568, 1515, 1363, 1188 (O=S=O) cm^{-1}; MS (EI): m/z (%) = 537 (10) [M^+], 365 (53) [M^+ – HOTs], 324 (100) [$M^+ - C_3H_6$OTs]; $C_{31}H_{27}N_3O_4S$ (537.6) calcd C 69.26, H 5.06, N 7.82; found C 69.02, H 4.96, N 7.72.

4′-[(3-(*p*-*tert*-Butylphenyl)propoxy)phenyl]-2,2′:6′,2″-terpyridine (12): A mixture of the tosylate **11** (200 mg, 0.40 mmol), 4-*tert*-butylphenol (60 mg, 0.40 mmol), and potassium carbonate (100 mg, 1.0 mmol) was refluxed in acetone (30 mL) for 3 d. The mixture was cooled and filtered. Concentration of the filtrate followed by flash chromatography on alumina (hexane/EtOAc = 2/300 gradient to 2/100) afforded **12** (0.14 g, 76%) as a white crystalline solid; m.p. 123–125 °C; R_f = 0.29 (hexane/$CHCl_3$ = 100/1.5); ^{1}H NMR ($CDCl_3$): δ = 8.72–8.63 (m, 4H), 8.70 (s, 2H), 7.87–7.82 (m, 4H), 7.33–7.26 (m, 2H), 7.29 (d, ^3J(H,H) = 8.8 Hz, 2H), 7.01 (d, ^3J(H,H) = 8.8 Hz, 2H), 6.87 (d, ^3J(H,H) = 8.8 Hz, 2H), 4.19 (t, ^3J(H,H) = 6.1 Hz, 2H; CH_2O), 4.15 (t, ^3J(H,H) = 6.0 Hz, 2H; CH_2O), 2.26 (quin, ^3J(H,H) = 6.1 Hz, 2H; CCH_2C), 1.29 (s, 9H, *t*Bu); ^{13}C NMR ($CDCl_3$): δ = 159.9, 156.6, 156.4, 155.8, 149.7, 149.0, 143.5, 136.7, 130.8, 128.4, 126.2, 123.6, 121.3, 118.2, 115.0, 114.1, 64.7 (OCH_2), 64.4 (OCH_2), 34.0 (CMe_3), 31.5 (CH_3), 29.4 (CCH_2C); IR (film): $\tilde{\nu}$ = 1608, 1584, 1567, 1514 cm^{-1}; MS (L-SIMS): m/z (%) = 516.3 (100) [$M + H^+$].

G0 (1): A mixture of the tosylate **11** (0.50 g, 1.0 mmol), **5** [11] (0.60 g, 1.0 mmol), and potassium carbonate (0.30 g, 2.2 mmol) was refluxed in acetone (50 mL) for 4 d. The mixture was cooled and filtered. The filtrate was evaporated in vacuo to give the crude compound. Flash chromatography on alumina (hexane/$CHCl_3$ = 10/3) afforded the terpyridine **1** (0.70 g, 80%) as a glassy white substance; R_f = 0.24 (hexane/$CHCl_3$ = 10/3); ^{1}H NMR ($CDCl_3$): δ = 8.74–8.64 (m, 4H), 8.71 (s, 2H), 7.90–7.82 (m, 4H), 7.34 (ddd, ^3J(H,H) = 7.4 Hz, ^3J(H,H) = 4.8 Hz and ^4J(H,H) = 1.1 Hz, 2H), 7.28 (d, ^3J(H,H) = 8.8 Hz, 4H), 7.03 (d, ^3J(H,H) = 8.8 Hz, 2H), 6.84 (d, ^3J(H,H) = 8.8 Hz, 4H), 6.11 (brs, 3H), 4.20 (t, ^3J(H,H) = 6.2 Hz, 2H; CH_2O), 4.16–4.07 (m, 10H; 5CH_2O), 2.30–2.15 (m, 6H; 3CCH_2C), 1.28 (s, 18H; 2*t*Bu); ^{13}C NMR ($CDCl_3$): δ = 160.7, 159.8, 156.5, 156.3, 155.8, 149.6, 149.0, 143.3, 136.6, 130.7, 128.4, 126.1, 123.6, 121.2, 118.1, 114.9, 114.0, 94.2, 64.5 (OCH_2), 64.4 (OCH_2), 64.3 (OCH_2), 33.9 (CMe_3), 31.4 (CH_3), 29.3 (CCH_2C); IR (film): $\tilde{\nu}$ = 2962, 1605, 1584, 1568, 1514 cm^{-1}; MS (L-SIMS): m/z (%) = 872.5 (100) [$M + H^+$]; $C_{56}H_{61}N_3O_6$ (872.1) calcd C 77.12, H 7.05, N 4.82; found C 76.64, H 7.03, N 4.76.

G1 (2): A mixture of the tosylate **11** (0.16 g, 0.30 mmol), **6** [11] (0.38 mg, 0.30 mmol), and potassium carbonate (0.10 g, 0.70 mmol) was refluxed in acetone/DMF (30 mL, 9/1) for 3 d. The mixture was cooled, filtered, and concentrated in vacuo to give the crude product. Flash chromatography on alumina (hexane/$CHCl_3$ = 20/7) afforded the terpyridine **2** (0.46 g, 96%) as a glassy white substance; R_f = 0.19 (hexane/$CHCl_3$ = 10/3); ^{1}H NMR ($CDCl_3$): δ = 8.75–8.65 (m, 4H), 8.73 (s, 2H), 7.93–7.84 (m, 4H), 7.35 (ddd, ^3J(H,H) = 7.4 Hz, ^3J(H,H) = 4.7 Hz and ^4J(H,H) = 1.1 Hz, 2H), 7.28 (d, ^3J(H,H) = 8.9 Hz, 8H), 7.03 (d, ^3J(H,H) = 8.8 Hz, 2H), 6.83 (d, ^3J(H,H) = 8.9 Hz, 8H), 6.14–6.10 (m, 3H), 6.08 (s, 6H), 4.20 (t, ^3J(H,H) = 5.9 Hz, 2H; CH_2O), 4.13–4.05 (m, 26H; 13CH_2O), 2.27–2.17 (m, 14H; 7CCH_2C), 1.28 (s, 36H; 4*t*Bu); ^{13}C NMR ($CDCl_3$): δ = 160.8, 159.9, 156.7, 156.5, 155.9, 149.8, 149.1, 143.5, 136.8, 130.8, 128.5, 126.2, 123.7, 121.4, 118.4, 115.0, 114.1, 94.4, 64.7 (OCH_2), 64.5 (OCH_2), 34.0 (CMe_3), 31.5 (CH_3), 29.7, 29.4; IR (film): $\tilde{\nu}$ = 1601, 1569, 1515 cm^{-1}; MS (L-SIMS): m/z (%) = 1585.0 (47) [$M + H^+$]; $C_{100}H_{117}N_3O_{14}$ (1585.1) calcd C 75.78, H 7.44, N 2.65; found C 75.51, H 7.51, N 2.70.

G2 (3): A mixture of the tosylate **11** (0.11 g, 0.20 mmol), **7** [11] (0.51 g, 0.20 mmol), and potassium carbonate (0.10 g, 0.70 mmol) was refluxed in acetone/DMF (35 mL, 6/1) for 2 d. The mixture was cooled, filtered, and concentrated in vacuo to give the crude product. Flash chromatography on alumina (hexane/$CHCl_3$ = 5/2) afforded **3** (0.52 g, 90%) as a glassy white substance; R_f = 0.19 (hexane/$CHCl_3$ = 5/2); ^{1}H NMR ($CDCl_3$): δ = 8.80–8.68 (m, 4H), 8.77 (s, 2H), 7.96–7.87 (m, 4H), 7.42–7.35 (m, 2H), 7.27 (d, ^3J(H,H) = 8.8 Hz, 16H), 7.03 (d, ^3J(H,H) = 8.8 Hz, 2H), 6.83 (d, ^3J(H,H) = 8.8 Hz, 16H), 6.12–6.07 (m, 21H), 4.24–4.03 (m, 60H; 30CH_2O), 2.25–2.15 (m, 30H; 15CCH_2C), 1.28 (s, 72H; 8*t*Bu); ^{13}C NMR ($CDCl_3$): δ = 160.8, 159.9, 156.6, 156.4, 155.8, 149.7, 149.0, 143.4, 136.7, 130.8, 128.5, 126.1, 123.6, 121.3, 118.3, 115.0, 114.0, 94.3, 64.6 (OCH_2), 34.0 (CMe_3), 31.5 (CH_3), 29.6, 29.3; IR (film): $\tilde{\nu}$ = 2961, 2877, 1600, 1550, 1514 cm^{-1}; MS (L-SIMS): m/z (%) = 3009.8 (7) [$M + H^+$]; $C_{188}H_{229}N_3O_{30}$ (3010.9) calcd C 75.00, H 7.67, N 1.40; found C 74.80, H 7.74, N 1.39.

G3 (4): A mixture of the tosylate **11** (15 mg, 0.027 mmol), **8** [11] (0.15 g, 0.027 mmol), and potassium carbonate (0.10 g, 0.70 mmol) was refluxed in acetone/DMF (30 mL, 5/1) for 32 h. The mixture was cooled and filtered. After concentration of the filtrate, the residue was redissolved in dichloromethane (30 mL) and washed with water (2 × 10 mL). The organic portion was dried, filtered, and evaporated in vacuo to give the crude compound. Flash chromatography on alumina (hexane/$CHCl_3$ = 5/2) afforded **4** (0.14 g, 89%) as a glassy white substance; R_f = 0.26 (hexane/$CHCl_3$ = 1/1); ^{1}H NMR ($CDCl_3$): δ = 8.74–8.64 (m, 4H), 8.72 (s, 2H), 7.89–7.83 (m, 4H), 7.38–7.30 (m, 2H), 7.26 (d, ^3J(H,H) = 8.8 Hz, 32H), 7.01 (d, ^3J(H,H) = 8.7 Hz, 2H), 6.82 (d, ^3J(H,H) = 8.8 Hz, 32H), 6.07 (brs, 45H), 4.11–4.04 (m, 124H; 62CH_2O), 2.21–2.14 (m, 62H; 31CCH_2C), 1.27 (s, 144H; 16*t*Bu); ^{13}C NMR ($CDCl_3$): δ = 160.9, 159.9, 156.7, 156.5, 156.0, 149.7, 149.1, 143.5, 136.7, 131.0, 128.5, 126.2, 123.6, 121.3, 118.3, 115.1, 114.2, 94.5, 64.7

0947-6539/96/0209-1090 $ 15.00+.25/0 Chem. Eur. J. 1996, 2, No. 9

(OCH_2), 64.6 (OCH_2), 34.0 (CMe_3), 31.5 (CH_3), 29.5, 29.4; IR (film): $\tilde{\nu}$ = 2961, 2877, 1601, 1514 cm^{-1}; MS (ESI): *m/z* (%) = 5859.2 (20) $[M+H^+]$; $C_{364}H_{453}N_3O_{62}$ (5862.7) calcd C 74.57, H 7.79, N 0.72; found C 74.36, H 7.83, N 0.83.

$[Fe(12)_2][PF_6]_2$ (13): $FeCl_2 \cdot 4H_2O$ (11.5 mg, 0.06 mmol) was added to a boiling methanolic solution (10.0 mL) of the terpyridine **12** (60.0 mg, 0.12 mmol), and a deep purple solution formed immediately. After the mixture had been refluxed for a further 30 min, a methanolic solution of NH_4PF_6 (20.0 mg, 0.12 mmol) was added. The precipitate was filtered and washed with methanol (30 mL) to give the iron complex **13** (42.0 mg, 67%) as a deep purple crystalline solid, m.p. > 278 °C; ^1H NMR ([D$_6$]acetone): δ = 9.57 (s, 4H), 9.00 (d, ^3J(H,H) = 7.9 Hz, 4H), 8.43 (d, ^3J(H,H) = 8.8 Hz, 4H), 8.03 (dt, ^4J(H,H) = 1.3 Hz and ^3J(H,H) = 7.8 Hz, 4H), 7.55 (d, ^3J(H,H) = 5.2 Hz, 4H), 7.37 (d, ^3J(H,H) = 8.6 Hz, 4H), 7.34 (d, ^3J(H,H) = 8.9 Hz, 4H), 7.23 (ddd, ^3J(H,H) = 7.2 Hz, ^3J(H,H) = 5.7 Hz and ^4J(H,H) = 1.2 Hz, 4H), 6.92 (d, ^3J(H,H) = 8.9 Hz, 4H), 4.41 (t, ^3J(H,H) = 6.2 Hz, 4H; $2CH_2O$), 4.24 (t, ^3J(H,H) = 6.1 Hz, 4H; $2CH_2O$), 2.34 (quin, ^3J(H,H) = 6.1 Hz, 4H; $2CCH_2C$) and 1.28 (s, 18H; 2*t*Bu); ^{13}C NMR (CD_3CN): δ = 162.1, 160.9, 158.8, 157.4, 153.7, 150.8, 144.2, 139.3, 130.0, 129.4, 127.8, 126.9, 124.3, 121.5, 116.4, 114.8, 65.9 (OCH_2), 65.2 (OCH_2), 34.3 (CMe_3), 31.4 (CH_3), 29.7 (CCH_2C); IR (film): $\tilde{\nu}$ = 1605 and 1515 cm^{-1}; MS (L-SIMS): *m/z* (%) = 1086.5 (15) $[(M-2PF_6)^+]$ and 543.3 (67) $[(M-2PF_6)^{2+}]$.

$[Fe(1)_2][PF_6]_2$ (14): $FeCl_2 \cdot 4H_2O$ (7.9 mg, 0.04 mmol) was added to a boiling methanolic solution (10 mL) of the terpyridine **1** (70 mg, 0.08 mmol) and a deep purple solution formed immediately. After the mixture had been refluxed for a further 2 h, a methanolic solution of NH_4PF_6 (13 mg, 0.080 mmol) was added. The mixture was allowed to cool to room temperature. The precipitate was filtered and washed with methanol (20 mL) to give the iron complex **14** (52 mg, 65%) as a deep purple crystalline solid, m.p. > 280 °C; ^1H NMR ([D$_6$]acetone): δ = 9.56 (s, 4H), 8.98 (d, ^3J(H,H) = 8.0 Hz, 4H), 8.43 (d, ^3J(H,H) = 8.8 Hz, 4H), 8.02 (t, ^3J(H,H) = 7.8 Hz, 4H), 7.54 (d, ^3J(H,H) = 5.3 Hz, 4H), 7.36 (d, ^3J(H,H) = 8.8 Hz, 4H), 7.29 (d, ^3J(H,H) = 8.8 Hz, 8H), 7.27–7.19 (m, 4H), 6.86 (d, ^3J(H,H) = 8.8 Hz, 8H), 6.19 (s, 6H), 4.39 (t, ^3J(H,H) = 6.2 Hz, 4H; $2CH_2O$), 4.22 (t, ^3J(H,H) = 6.1 Hz, 4H; $2CH_2O$), 4.19–4.10 (m, 16H), 2.32 (quin, ^3J(H,H) = 6.3 Hz, 4H; $2CCH_2C$), 2.20 (quin, ^3J(H,H) = 6.2 Hz, 8H; $4CCH_2C$), 1.24 (s, 36H; 4*t*Bu); ^{13}C NMR ($CDCl_3$): δ = 161.2, 160.9, 160.8, 159.9, 157.8, 156.6, 152.6, 151.0, 143.5, 138.6, 129.6, 128.6, 127.6, 126.2, 123.8, 120.8, 115.8, 114.1, 94.5, 64.8 (OCH_2), 64.6 (OCH_2), 34.0 (CMe_3), 31.5 (CH_3), 29.7 (CCH_2C), 29.4 (CCH_2C); IR (film): $\tilde{\nu}$ = 1602 and 1514 cm^{-1}; MS (L-SIMS): *m/z* (%) = 1798.9 (55) $[(M-HPF_6-PF_6)^+]$ and 899.4 (82) $[(M-2PF_6)^{2+}]$; $C_{112}H_{122}N_6O_{12}FeP_2F_{12}$ (2090.0) calcd C 64.37, H 5.88, N 4.02; found C 63.88, H 5.85, N 3.93.

$[Fe(2)_2][PF_6]_2$ (15): A methanolic solution of $FeCl_2 \cdot 4H_2O$ (2.8 mg, 0.014 mmol) was added to a boiling solution of G1 **2** (45 mg, 0.028 mmol) in ethanol/$CHCl_3$ (9 mL, 2/1) mixture. After the mixture had been refluxed for a further 2 h, a methanolic solution of NH_4PF_6 (4.5 mg, 0.028 mmol) was added and the mixture was cooled to room temperature. The precipitate was filtered and purified by flash chromatography on alumina (hexane/$CHCl_3$ = 1/1 followed by $CHCl_3$/ethanol = 4/1) to give the iron complex **15** (37 mg, 82%) as a deep purple amorphous solid; m.p. > 280 °C; ^1H NMR ([D$_6$]acetone): δ = 9.55 (s, 4H), 8.96 (d, ^3J(H,H) = 8.0 Hz, 4H), 8.42 (d, ^3J(H,H) = 8.7 Hz, 4H), 8.00 (t, ^3J(H,H) = 6.6 Hz, 4H), 7.52 (d, ^3J(H,H) = 5.2 Hz, 4H), 7.35 (d, ^3J(H,H) = 8.7 Hz, 4H), 7.26 (d, ^3J(H,H) = 8.9 Hz, 16H), 7.23–7.18 (m, 4H), 6.83 (d, ^3J(H,H) = 8.8 Hz, 16H), 6.18 (s, 6H), 6.14 (s, 12H), 4.38 (t, ^3J(H,H) = 6.1 Hz, 4H; $2CH_2O$), 4.21 (t, ^3J(H,H) = 5.7 Hz, 4H; $2CH_2O$), 4.15–4.05 (m, 48H), 2.31 (quin, ^3J(H,H) = 5.4 Hz, 4H; $2CCH_2C$), 2.22–2.11 (m, 24H; $12CCH_2C$), 1.23 (s, 72H; 8*t*Bu); ^{13}C NMR ($CDCl_3$): δ = 161.3, 160.8, 159.8, 157.7, 156.6, 152.6, 151.0, 143.5, 138.6, 129.5, 128.6, 127.6, 126.2, 123.7, 120.7, 115.8, 114.1, 94.4, 64.7 (OCH_2), 64.5 (OCH_2), 34.0 (CMe_3), 31.5 (CH_3), 29.4 (CCH_2C); IR (film): $\tilde{\nu}$ = 2960, 2853, 1602, 1515 cm^{-1}; MS (L-SIMS): *m/z* (%) = 3224.1 (12) $[(M-2PF_6)^+]$ and 1611.9 (27) $[(M-2PF_6)^{2+}]$; $C_{200}H_{234}N_6O_{28}FeP_2F_{12}$ (3515.9) calcd C 68.32, H 6.71, N 2.39; found C 68.41, H 6.75, N 2.38.

$[Fe(3)_2][PF_6]_2$ (16): A methanolic solution of $FeCl_2 \cdot 4H_2O$ (2.6 mg, 0.014 mmol) was added to a boiling solution of G2 **3** (82 mg, 0.027 mmol) in ethanol/$CHCl_3$ (9 mL, 2/1) mixture and a deep purple solution formed immediately. After the mixture had been refluxed for a further 1 h, a methanolic solution of NH_4PF_6 (4.4 mg, 0.027 mmol) was added. The mixture was cooled to room temperature. The solution was decanted and the purple residue rinsed with methanol (3 × 5 mL). The crude product was purified by flash chromatography on alumina (hexane/EtOAc = 2/1 followed by $CHCl_3$/ethanol = 4/1) to give the complex **16** (69 mg, 79%) as deep purple amorphous solid; m.p. > 80 °C; ^1H NMR ([D$_6$]acetone): δ = 9.53 (s, 4H), 8.93 (d, ^3J(H,H) = 8.1 Hz, 4H), 8.41 (d, ^3J(H,H) = 8.9 Hz, 4H), 7.97 (t, ^3J(H,H) = 5.6 Hz, 4H), 7.50 (d, ^3J(H,H) = 5.3 Hz, 4H), 7.34 (d, ^3J(H,H) = 8.8 Hz, 4H), 7.25 (d, ^3J(H,H) = 8.9 Hz, 32H), 7.21–7.14 (m, 4H), 6.81 (d, ^3J(H,H) = 8.9 Hz, 32H), 6.17 (s, 6H), 6.11 (brs, 36H), 4.36–4.33 (m, 4H; $2CH_2O$), 4.18–4.04 (m, 116H; $58CH_2O$), 2.32–2.27 (m, 4H; $2CCH_2C$), 2.19–2.07 (m, 56H; $28CCH_2C$), 1.22 (s, 144H; 16*t*Bu); ^{13}C NMR ($CDCl_3$): δ = 161.5, 160.9, 159.9, 157.8, 156.7, 152.8, 151.3, 143.5, 138.6, 129.5, 128.6, 127.7, 126.2, 123.7, 120.9, 116.0, 114.2, 94.5, 64.8 (OCH_2), 64.6 (OCH_2), 34.0 (CMe_3), 31.5 (CH_3), 29.5 (CCH_2C); IR (film): $\tilde{\nu}$ = 2961, 2877, 1601, 1514 cm^{-1}; MS (ESI): *m/z* (%) = 3038.6 [19] (100) $[(M-2PF_6)^{2+}]$; $C_{376}H_{458}N_6O_{60}FeP_2F_{12}$ (6367.6) calcd C 70.92, H 7.25, N 1.32; found C 70.51, H 7.30, N 1.30.

$[Fe(4)_2][PF_6]_2$ (17): A methanolic solution of $FeCl_2 \cdot 4H_2O$ (1.7 mg, 0.0085 mmol) was added to a boiling solution of G3 **4** (100 mg, 0.017 mmol) in ethanol/$CHCl_3$ (8 mL, 1/1) mixture and a deep purple solution formed immediately. After the mixture had refluxed for 2 h, a methanolic solution of NH_4PF_6 (3.0 mg, 0.018 mmol) was added. The mixture was cooled to room temperature. The solution was decanted and the purple gel-like residue washed with methanol (3 × 5 mL). The crude product was purified by flash chromatography on alumina (hexane/EtOAc = 2/1 followed by $CHCl_3$/ethanol 4/1) to give the iron complex **17** (83 mg, 80%) as a purple amorphous solid; m.p. > 280 °C; ^1H NMR ([D$_6$]acetone): δ = 9.49 (s, 4H), 8.87 (d, ^3J(H,H) = 7.9 Hz, 4H), 8.40 (d, ^3J(H,H) = 7.3 Hz, 4H), 7.92 (t, ^3J(H,H) = 7.4 Hz, 4H), 7.46 (d, ^3J(H,H) = 6.2 Hz, 4H), 7.33–7.30 (m, 4H), 7.22 (d, ^3J(H,H) = 8.8 Hz, 64H), 7.19–7.12 (m, 4H), 6.79 (d, ^3J(H,H) = 8.8 Hz, 64H), 6.15 (s, 6H), 6.10 (brs, 84H), 4.35–4.27 (m, 4H), 4.15–3.95 (m, 244H; $122CH_2O$), 2.30–2.22 (m, 4H), 2.18–2.05 (m, 120H; $60CCH_2C$), 1.20 (s, 288H; 32*t*Bu); ^{13}C NMR ($CDCl_3$): δ = 161.5, 160.8, 159.8, 157.7, 156.6, 152.8, 151.3, 143.4, 138.6, 129.5, 128.5, 127.7, 126.1, 123.6, 120.9, 116.0, 114.1, 94.4, 64.7 (OCH_2), 64.5 (OCH_2), 34.0 (CMe_3), 31.5 (CH_3), 29.4 (CCH_2C); IR (film): $\tilde{\nu}$ = 2963, 1601, 1514 cm^{-1}; MS (ESI): *m/z* (%) = 5891.2 [20] (61) $[(M-2PF_6)^{2+}]$; $C_{728}H_{906}N_6O_{124}FeP_2F_{12}$ (12071.1) calcd C 72.44, H 7.57, N 0.70; found C 72.12, H 7.60, N 0.87.

Acknowledgments: This work was supported by the Research Grants Council, HK, and a Direct Grant from the Physical Science Panel, CUHK, HK.

Received: April 2, 1996 [F344]

[1] For reviews, see a) D. A. Tomalia, A. M. Naylor, W. A. Goddard III, *Angew. Chem.* **1990**, *102*, 119; *Angew. Chem. Int. Ed. Engl.* **1990**, *29*, 138; b) G. R. Newkome, C. N. Moorefield, G. R. Baker, *Aldrichim. Acta* **1992**, *25*, 31; c) J. M. J. Fréchet, *Science* **1994**, *263*, 1710.

[2] J. Issberner, R. Moors, F. Vögtle, *Angew. Chem.* **1994**, *106*, 2507; *Angew. Chem. Int. Ed. Engl.* **1994**, *33*, 2413.

[3] a) G. Caminati, N. J. Turro, D. A. Tomalia, *J. Am. Chem. Soc.* **1990**, *112*, 8515; b) S. Campagna, G. Denti, S. Serroni, A. Juris, M. Venturi, V. Ricevuto, V. Balzani, *Chem. Eur. J.* **1995**, *1*, 211; c) R.-H. Jin, T. Aida, S. Inoue, *J. Chem. Soc. Chem. Commun.* **1993**, 1260.

[4] a) P. J. Dandliker, F. Diederich, M. Gross, C. B. Knobler, A. Louati, E. M. Sanford, *Angew. Chem.* **1994**, *106*, 1821; *Angew. Chem. Int. Ed. Engl.* **1994**, *33*, 1739; b) G. R. Newkome, R. Güther, C. N. Moorefield, F. Cardullo, L. Echegoyen, E. Pérez-Cordero, H. Luftmann, *ibid.* **1995**, *107*, 2159 and **1995**, *34*, 2023; c) P. J. Dandliker, F. Diederich, J.-P. Gisselbrecht, A. Louati, M. Gross, *ibid.* **1995**, *107*, 2906 and **1995**, *34*, 2725.

[5] a) D. Seebach, J.-M. Lapierre, K. Skobridis, G. Greiveldinger, *Angew. Chem.* **1994**, *106*, 457; *Angew. Chem. Int. Ed. Engl.* **1994**, *33*, 440; b) H.-F. Chow, L. F. Fok, C. C. Mak, *Tetrahedron Lett.* **1994**, *35*, 3547; c) J. F. G. A. Jansen, H. W. I. Peerings, E. M. M. de Brabander-van den Berg, E. W. Meijer, *Angew. Chem.* **1995**, *107*, 1321; *Angew. Chem. Int. Ed. Engl.* **1995**, *34*, 1206.

[6] a) T. Nagasaki, O. Kimura, M. Ukon, S. Arimori, I. Hamachi, S. Shinkai, *J. Chem. Soc. Perkin Trans. 1* **1994**, 75; b) J. F. G. A. Jansen, E. M. M. de Brabander-van den Berg, E. W. Meijer, *Science* **1994**, *266*, 1226; c) J. F. G. A. Jansen, E. W. Meijer, E. M. M. de Brabander-van den Berg, *J. Am. Chem. Soc.* **1995**, *117*, 4417; d) S. Mattei, P. Seiler, F. Diederich, V. Gramlich, *Helv. Chim. Acta* **1995**, *78*, 1904.

[7] a) H. Brunner, *J. Organomet. Chem.* **1995**, *500*, 39; b) J.-J. Lee, W. T. Ford, J. A. Moore, Y. Li, *Macromolecules* **1994**, *27*, 4632; c) A. Miedaner, C. J. Curtis, R. M. Barkley, D. L. DuBois, *Inorg. Chem.* **1994**, *33*, 5482; d) J. W. J. Knapen, A. W. van der Made, J. C. de Wilde, P. W. N. M. van Leeuwen, P. Wijkens, D. M. Grove, G. van Koten, *Nature* **1994**, *372*, 659.

[8] For a review, see S. K. Chapman, A. R. Mount, *Nat. Prod. Rep.* **1995**, 93.

[9] C. J. Hawker, J. M. J. Fréchet, *J. Am. Chem. Soc.* **1990**, *112*, 7638.

[10] a) G. R. Newkome, F. Cardullo, E. C. Constable, C. N. Moorefield, A. M. W. C. Thompson, *J. Chem. Soc. Chem. Commun.* **1993**, 925; b) E. C. Constable, P. Harverson, *Chem. Commun.* **1996**, 33.

[11] a) H.-F. Chow, I. Y.-K. Chan, C. C. Mak, *Tetrahedron Lett.* **1995**, *36*, 8633; b) H.-F. Chow, I. Y.-K. Chan, C. C. Mak, M.-K. Ng, *Tetrahedron* **1996**, *52*, 4277.

[12] W. Spahni, G. Calzaferri, *Helv. Chim. Acta* **1984**, *67*, 450.

[13] E. C. Constable, M. D. Ward, S. Corr, *Inorg. Chim. Acta* **1988**, *141*, 201.

[14] R. Hogg, R. G. Wilkins, *J. Chem. Soc.* **1962**, 341.

[15] D. E. Morris, K. W. Hanck, M. K. DeArmond, *J. Electroanal. Chem.* **1983**, *149*, 115.

[16] a) F. A. Armstrong, H. A. O. Hill, N. J. Walton, *Acc. Chem. Res.* **1988**, *21*, 407; b) H. A. O. Hill, *Pure Appl. Chem.* **1987**, *59*, 143.

[17] Y. Degani, A. Heller, *J. Phys. Chem.* **1987**, *91*, 1285.

[18] S. I. Stupp, J. S. Moore, EPA EP242278, **1987**; *Chem. Abstr.* **1988**, *108*, 159114k.

[19] Mass of most abundant isotopic peak.

[20] Average molecular mass.